

Physics Performance of a Low-Luminosity Low Energy Neutrino Factory

E. Christensen,¹ P. Coloma,¹ and P. Huber¹

¹*Center for Neutrino Physics, Virginia Tech, Blacksburg, VA 24061, USA*

(Dated: April 3, 2024)

We investigate the minimal performance, in terms of beam luminosity and detector size, of a neutrino factory to achieve a competitive physics reach for the determination of the mass hierarchy and the discovery of leptonic CP violation. We find that a low luminosity of 2×10^{20} useful muon decays per year and 5 GeV muon energy aimed at a 10 kton magnetized liquid argon detector placed at 1300 km from the source provides a good starting point. This result relies on θ_{13} being large and assumes that the so-called platinum channel can be used effectively. We find that such a minimal facility would perform significantly better than phase I of the LBNE project and thus could constitute a reasonable step towards a full neutrino factory.

PACS numbers: 14.60.Pq, 14.60.Lm

Keywords: neutrino oscillation, neutrino mixing, CP violation

The recent discovery of θ_{13} [1–3] is a major step towards the completion of the leptonic mixing matrix. The remaining unknown mixing parameters, within a three neutrino framework, are the Dirac CP-violating phase, δ , and the ordering of the neutrino mass eigenstates, $\text{sgn}(\Delta m_{31}^2)$. CP violation (CPV) within the Standard Model has proved to be quite intriguing in the hadronic sector already: even though the strong interaction seems to be conserving CP, it is significantly violated in quark mixing. Neutrinos now offer the third opportunity to learn more about the role of the CP symmetry in Nature. Also, if one considers the question of unitarity and the completeness of the three neutrino picture, the determination of the CP phase will play a crucial role, like it did in the quark sector.

Direct CPV in neutrino oscillations can only be observed in appearance experiments, where the initial and final neutrino flavors are different. For practical reasons, this requirement confines experiments to study $\nu_e \leftrightarrow \nu_\mu$ and $\bar{\nu}_e \leftrightarrow \bar{\nu}_\mu$ transitions. Conventional neutrino beams are obtained from the decay of relativistic pions and therefore predominantly consist of ν_μ or $\bar{\nu}_\mu$, depending on whether π^+ or π^- are selected at the beam source. The current generation of experiments employing this type of beam has a limited sensitivity to CPV, even if their results are combined [4].

Therefore, a number of new experiments has been proposed in order to observe CPV in the leptonic sector, see for instance Ref. [5]; in the U.S. context, this proposal is the long baseline neutrino experiment (LBNE). The first stage of the LBNE project comprises a 700 kW proton beam to produce pions and a 10 kton liquid argon (LAr) detector placed at a distance $L = 1300$ km from the source [6]. The CPV discovery potential is limited due to a lack of statistics, though. An upgraded beam in

the multi-MW range (superbeam) would obviously yield a much better physics potential [7]. However, these beams are eventually limited by intrinsic backgrounds and systematic effects: large flux uncertainties, combined with the inability to measure the final flavor cross sections at the near detector, introduce large systematical errors which are very difficult to control [8, 9].

For the determination of the CP phase a similar precision to that achieved in the quark sector is only offered by a neutrino factory (NF) [9, 10]. In a NF a highly collimated beam of muon neutrinos and electron antineutrinos is produced from muon decays in a storage ring with long straight sections [11]. Muon decays result in a beam with equal number of ν_μ and $\bar{\nu}_e$; the CP-conjugate beam is obtained from μ^+ decays. The main observables at the NF for μ^- decay are: $\bar{\nu}_e \rightarrow \bar{\nu}_\mu$, so-called golden channel [12]; and the $\nu_\mu \rightarrow \nu_\mu$ disappearance channel. At the detector, the signal is in both cases extracted from the charged-current interaction sample. Therefore, the electric charge of the muon needs to be identified in order to disentangle the appearance and disappearance signals. Charge identification typically is achieved by employing a magnetic field in 0.2-2 T range. Moreover, an appropriate detector and/or muon energy would allow to observe additional channels – $\nu_\mu \rightarrow \nu_e$ (platinum), $\nu_\mu \rightarrow \nu_\tau$ and $\nu_e \rightarrow \nu_\tau$ (silver), see for instance Refs. [13, 14].

The NF was originally proposed to operate at very high energies, $E_\mu \sim 25 - 50$ GeV, and optimized under the assumption of a very small θ_{13} , $\sin^2 2\theta_{13} \lesssim 10^{-3}$. However, it has recently been argued that a lower energy version would be better optimized for the large θ_{13} scenario and technically less demanding. Therefore, the present NF design parameters [15] are 10^{21} useful muon decays per 10^7 seconds, aimed to a 100 kton magnetized iron detector

(MIND) placed at 2000 km from the source, with a parent muon energy of 10 GeV. The performance of this setup is remarkable, and clearly superior to that of any conventional muon beam, see for instance Ref. [5]. However, in order to form an intense muon beam for acceleration and storage, muon phase space cooling is required for this default configuration. In addition, the fact that neutrinos in a NF are a tertiary beam implies significant proton driver intensities; in this case, a 4 MW proton beam together with its associated target station. These technical challenges are to be contrasted with the advantages of a NF – there are no intrinsic backgrounds and the absolute neutrino flux can be determined to much better than 1%. Furthermore, the presence of both muon and electron neutrinos in the beam does allow for a measurement of all final flavor cross sections at the near detector.

Recently, it has been suggested that a very low energy NF, now called nuSTORM [16], with greatly reduced beam power and a muon energy around 4 GeV, could be used for sterile neutrino searches as well as to perform neutrino cross section measurements in the low energy regime. Such a facility could well serve as a first stage towards a full NF. Nevertheless, in order to do long baseline oscillation studies, additional acceleration would be required to achieve enough statistics at the far detector. What we propose in this work is to use a neutrino beam which would lie in between nuSTORM and a full NF in terms of luminosity. Specifically, we study a configuration with a muon energy of 5 GeV and 10^{20} useful muon decays per year and polarity, which already implies a reduction of a factor of 10 over the luminosity usually considered for NF setups. The beam energy of 5 GeV is optimal for the considered distance of 1300 km since it balances the position of the oscillation maximum with the peak of the event distribution [17, 18]. The choice of the number of useful muon decays is inspired by a recent study based on Fermilab’s planned Project X accelerator complex [19]. Specifically, the number we use corresponds to a proton beam of 1 MW power at 3 GeV and does *not* assume any muon phase space cooling. As a result, most of the technical difficulties of a full NF can be avoided.

As already mentioned, a fundamental advantage of the NF with respect to other possible neutrino beams is the possibility to observe many oscillation channels using the same neutrino beam. The combination of CP- and CPT-conjugate channels not only provides crucial constraints for the observation of leptonic CP violation and/or effects coming from

	Channel	Effs.	Bg. Rej.	$\sigma(E_\nu)$	E_ν (GeV)
LAr	ν_μ	80%	99.9%	$0.2\sqrt{E}$	[0.5, 5]
	ν_e	80%	99%	$0.15\sqrt{E}$	[0.5, 5]
TASD	ν_μ	73%-94%	99.9%	$0.2\sqrt{E}$	[0.5, 5]
	ν_e	37%-47%	99%	$0.15\sqrt{E}$	[0.5, 5]

TABLE I: Main details used to simulate the LAr and TASD detector responses. The two rows correspond to the details used for ν_μ and ν_e detection. The different columns indicate: signal efficiencies, background rejection efficiencies (Neutral Current, Charge misID, Flavor misID), energy resolution and neutrino energy range. NC backgrounds have been migrated to lower energies using LBNE migration matrices [7].

new physics. It also helps to mitigate the effect from the matter density uncertainty [13], which constitutes the most relevant source of systematic uncertainties at a NF [9, 20]. Therefore, the simultaneous observation of both golden and platinum channels at a NF would yield extremely robust results, since they are CPT conjugates. However, the platinum channel is inaccessible in a MIND, because it requires to identify electron neutrino charged current events, and electric charge identification is again needed in this case in order to disentangle the ν_e appearance and $\bar{\nu}_e$ disappearance signals. The feasibility of electron charge identification was studied in Ref. [21] in the context of a low energy NF for a totally active scintillator detector (TASD) magnetized to 0.5 T using a so-called magnetic cavern. It soon was speculated that a magnetized LAr detector should be suitable as well [17, 22, 23].

In this work we consider a 10 kt magnetized LAr detector at a distance of 1300 km. This choice of detector size and baseline is obviously inspired by LBNE: it allows to reuse the LBNE facilities to the largest possible extent. Note, that the detector most likely will have to be deep underground due to the large duty factor of stored particle beams as in a NF. Tab. I summarizes the detector parameters used in this work. In the absence of a detailed study of the performance of a magnetized LAr detector, we have followed Refs. [7, 23]. The expected total event rates for a 10 kton LAr detector are shown in Tab. II. Since the LAr performance is indeed uncertain, we also evaluate sensitivities using the performance parameters of a TASD, which are based on simulation studies [21]. The same background migration matrices and energy resolution as for the LAr detector have been considered. Energy depen-

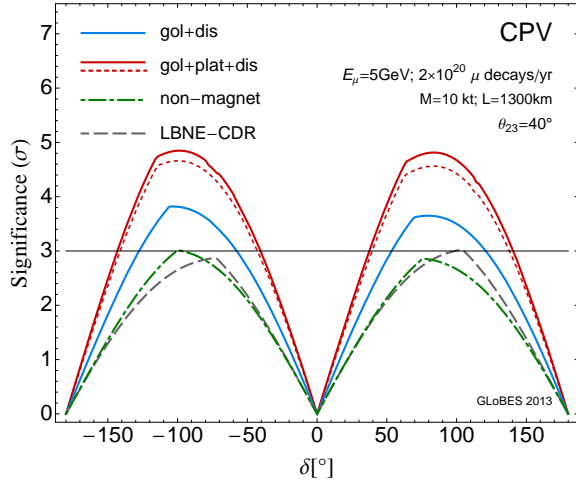


FIG. 1: CPV discovery potential as a function of the true value of δ . Results are shown for the combination of only the golden and ν_μ disappearance signals (blue lines, “gol+dis”), as well as when the platinum signal is also considered (red lines, “gol+dis+plat”). Solid (dotted) red lines show the results for a magnetized LAr (TASD) detector. Dot-dashed green lines show the results for a 10 kton non-magnetized LAr detector. For reference, the results for LBNE phase I are also shown (dashed gray lines).

dent efficiencies for the signal, following Ref. [23], have been used in this case, see Tab. I. In addition to the backgrounds considered in previous references, the τ -contamination [24–26] has also been included in this work. Systematic uncertainties have been implemented as in Ref. [9], using the default values listed in Tab. 2 therein.

Channel	$\nu_e \rightarrow \nu_\mu$	$\nu_\mu \rightarrow \nu_e$	$\nu_\mu \rightarrow \nu_\mu$
Signal	267	276	1485
Background	7	73	17
Channel	$\bar{\nu}_e \rightarrow \bar{\nu}_\mu$	$\bar{\nu}_\mu \rightarrow \bar{\nu}_e$	$\bar{\nu}_\mu \rightarrow \bar{\nu}_\mu$
Signal	52	59	562
Background	6	73	6

TABLE II: Expected total number of events for the low luminosity NF aiming to a 10 kton LAr detector, for $\sin^2 2\theta_{13} = 0.1$ and $\delta = 0$. The experiment is assumed to run with both polarities circulating in the ring at the same time, for 10 years. This results in a total of 2×10^{21} muon decays in the straight sections of the storage ring (half per polarity). Signal and background rejection efficiencies are already accounted for.

Figure 1 shows the results for the CPV discovery potential of the facility, defined as the ability of the

experiment to rule out the CP conservation hypothesis ($\delta = 0, \pi$). The statistical significance of the signal is shown as a function of the true value of δ . For reference, we also show the results for phase I of the LBNE experiment, which has been simulated according to the CDR from October 2012, Ref. [6]. It should be noted that for the LBNE results systematic uncertainties have been implemented as overall normalization errors over all signal and background contributions at once (no near detector has been simulated for this setup). Clearly, the low energy, low luminosity NF outperforms LBNE by a considerable margin, and the results combining only the golden and disappearance signals are already better; as expected, if the platinum signal is added then the performance is considerably improved. If magnetization of a massive LAr were not possible, several methods would in principle allow to statistically differentiate the charge of the leptons produced at a LAr detector, see for instance Ref. [27]. Therefore, we also show in Fig. 1 the performance of the setup using a non-magnetized LAr detector, simulated following Ref. [27] (dot-dashed green lines). We assume that $\nu/\bar{\nu}$ separation at the 90% (70%) for μ -like (e -like) events can be obtained for a non-magnetized LAr detector. Regarding the MH discovery potential, we find that a low luminosity NF combined with a LAr (TASD) detector can rule out the wrong hierarchy at $\sim 10\sigma$ (8σ) CL for 1 d.o.f., regardless of the true value of δ . It should be kept in mind that LBNE phase I would reach 3σ (5σ) CL for approximately 75% (50%) of the values of δ [6].

The left panel in Fig. 2 shows the allowed region in θ_{13} - δ plane for one particular point in the parameter space, where the different line styles correspond to different combinations of channels. Clearly, the addition of the platinum channel improves the performance beyond a mere increase of statistics – a true synergy, whose origin is explained in Ref. [13]. The right hand panel, on the other hand, shows the achievable precision for a measurement of δ at 1σ as a function of the true value of δ . Again, we find that the low luminosity low energy NF constitutes a marked improvement over LBNE. We also show in this case a green band, which corresponds to the results using a 10 kton non-magnetized LAr detector. The lower limit in the band corresponds to the case where a $\nu/\bar{\nu}$ separation of 90% (70%) is considered for μ -like (e -like) events, as in Fig. 1; the upper limit corresponds to the case when the separation for μ -like events is reduced down to 70%.

We would also like to point out that, once a 4 MW 8 GeV proton beam becomes available from

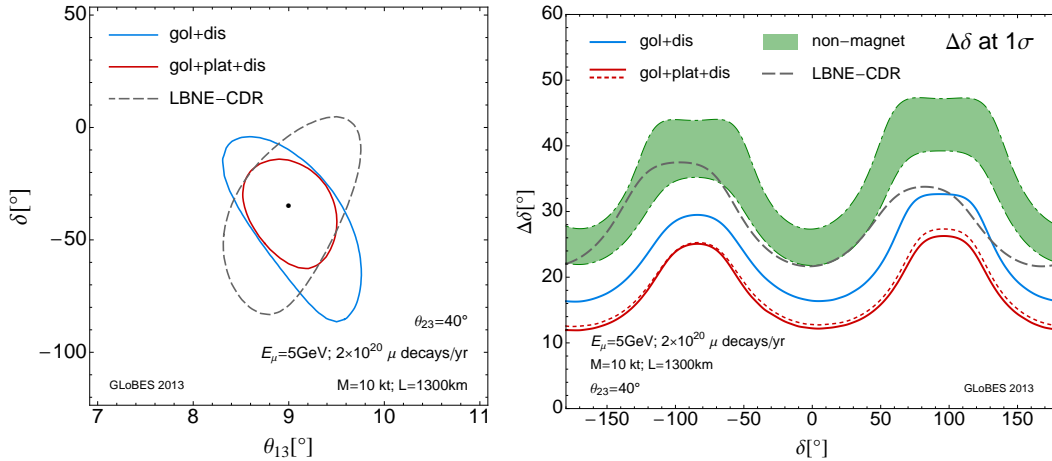


FIG. 2: Left panel: confidence region in the $\theta_{13} - \delta$ plane for a particular point in the parameter space, at 1σ CL (2 d.o.f.). Right panel: precision achievable for a measurement in δ at the 1σ CL (1 d.o.f.), as a function of the true value of δ . Results are shown when only the golden and disappearance channels are included in the analysis (blue lines, “gol+dis”), as well as when the platinum channel is also considered (red lines, “gol+dis+plat”). Solid (dotted) red lines show the results for a magnetized LAr (TASD) detector. The green bands show the physics reach for a 10 kton non-magnetized LAr detector, see text for details. For reference, the results for LBNE phase I are also shown (dashed gray lines).

Project X, muon cooling is added and the detector mass is increased by a factor 1-3, the performance of this facility reaches the 5° -level in CP accuracy, comparable to the baseline NF. Therefore, neither the initial energy of 5 GeV nor the baseline do need to be changed in later stages.

In summary, using 10 times less useful muon decays and a 10 times smaller detector mass with respect to the baseline NF still allows a muon decay based neutrino beam to outperform realistic conventional beams like LBNE phase I, while offering at the same time the path to a full scale NF. Such low luminosity can be achieved using existing proton drivers and without muon cooling. The reduced muon energy makes it possible to use a shorter baseline around 1300 km, and the use of a magnetized LAr detector allows to fully exploit the physics potential of the platinum channel, which is crucial for the overall performance of the facility. These choices for baseline and detector technology ensure a good synergy with the first stage of a superbeam program. The big open question is how well can a LAr detector perform this task.

This work has been supported by the U.S. Department of Energy under award number DE-SC0003915. We would like to thank M. Bishai and M. Bass for helping us to reproduce the LBNE sensitivities.

-
- [1] F. An et al. (Daya Bay Collaboration), *Chin. Phys.* **C37**, 011001 (2013), 1210.6327.
 - [2] J. Ahn et al. (RENO collaboration), *Phys.Rev.Lett.* **108**, 191802 (2012), 1204.0626.
 - [3] Y. Abe et al. (Double Chooz Collaboration), *Phys.Rev.* **D86**, 052008 (2012), 1207.6632.
 - [4] P. Huber, M. Lindner, T. Schwetz, and W. Winter, *JHEP* **0911**, 044 (2009), 0907.1896.
 - [5] S. Agarwalla, E. Akhmedov, M. Blennow, P. Coloma, A. Donini, et al. (2012), 1209.2825.
 - [6] LBNE Conceptual Design Report from Oct 2012, volume 1, URL <https://sharepoint.fnal.gov/project/lbne/LBNE%20at%20Work/SitePages/Reports%20and%20Documents.aspx>.
 - [7] T. Akiri et al. (LBNE Collaboration) (2011), 1110.6249.
 - [8] P. Huber, M. Mezzetto, and T. Schwetz, *JHEP* **0803**, 021 (2008), 0711.2950.
 - [9] P. Coloma, P. Huber, J. Kopp, and W. Winter (2012), 1209.5973.
 - [10] P. Coloma, A. Donini, E. Fernandez-Martinez, and P. Hernandez, *JHEP* **1206**, 073 (2012), 1203.5651.
 - [11] S. Geer, *Phys.Rev.* **D57**, 6989 (1998), hep-ph/9712290.
 - [12] A. Cervera, A. Donini, M. Gavela, J. Gomez Cadenas, P. Hernandez, et al., *Nucl.Phys.* **B579**, 17 (2000), hep-ph/0002108.
 - [13] P. Huber, M. Lindner, M. Rolinec, and W. Winter, *Phys.Rev.* **D74**, 073003 (2006), hep-ph/0606119.
 - [14] A. Donini, D. Meloni, and P. Migliozi, *Nucl.Phys.* **B646**, 321 (2002), hep-ph/0206034.
 - [15] S. Choubey et al. (IDS-NF Collaboration) (2011),

- 1112.2853.
- [16] P. Kyberd et al. (nuSTORM Collaboration) (2012), 1206.0294.
 - [17] P. Ballett and S. Pascoli, Phys.Rev. **D86**, 053002 (2012), 1201.6299.
 - [18] J. Tang and W. Winter, Phys.Rev. **D81**, 033005 (2010), 0911.5052.
 - [19] Muon Accelerator Program, *Muon accelerator program snowmass whitepaper* (2013), in preparation.
 - [20] P. Huber, M. Lindner, and W. Winter, Nucl.Phys. **B645**, 3 (2002), hep-ph/0204352.
 - [21] A. D. Bross, M. Ellis, S. Geer, O. Mena, and S. Pascoli, Phys.Rev. **D77**, 093012 (2008), 0709.3889.
 - [22] P. Kyberd, M. Ellis, A. Bross, S. Geer, O. Mena, et al. (2009), FERMILAB-FN-0836-APC.
 - [23] E. Fernandez Martinez, T. Li, S. Pascoli, and O. Mena, Phys.Rev. **D81**, 073010 (2010), 0911.3776.
 - [24] D. Indumathi and N. Sinha, Phys.Rev. **D80**, 113012 (2009), 0910.2020.
 - [25] A. Donini, J. Gomez Cadenas, and D. Meloni, JHEP **1102**, 095 (2011), 1005.2275.
 - [26] R. Dutta, D. Indumathi, and N. Sinha, Phys.Rev. **D85**, 013003 (2012), 1103.5578.
 - [27] P. Huber and T. Schwetz, Phys.Lett. **B669**, 294 (2008), 0805.2019.